EFFECTS OF POST-FAILURE MODELLING ON THE RESPONSE OF BALLISTICALLY IMPACTED COMPOSITES

Jack van Hoof [1], Michael J. Worswick [2], Paul V. Straznicky [1], and Manon Bolduc [3]

[1] *Department of Mechanical and Aerospace Engineering, Carleton University, 1125 Colonel By Drive, Ottawa, Ontario, K1S 5B6, Canada*
[2] *Department of Mechanical Engineering, University of Waterloo, Waterloo, Ontario, N2L 3G1, Canada*
[3] *Defence Research Establishment Valcartier, 2459 Pie XI Blvd. North, Val-Belair, Quebec, G3J 1X5, Canada*

SUMMARY: A numerical model incorporating the major energy dissipation mechanisms in ballistically impacted composites (through-thickness compressive and shear failure, fibre breakage, matrix cracking, and delamination) was implemented as a user-defined material subroutine in the LS-DYNA finite element code. Post-failure response was simulated for the various failure modes using a continuum damage mechanics approach. Penetration and backplane deformation due to a 1.1 g fragment simulating projectile (FSP) impacting at velocities ranging between 400-600 m/s was predicted for flat aramid fabric-reinforced composite panels. The effects of post-failure modelling on the penetration and backplane response were investigated.

KEYWORDS: post-failure, ballistic impact, delamination, continuum damage mechanics, numerical simulation.

INTRODUCTION

Laminated composites fabricated from high-performance polymeric fibres, such as polyethylene and aramid, provide essential characteristics for ballistic head protection purposes including light-weight, high strength, damage tolerance, and tailorability. The performance of composite laminates under ballistic impact is generally measured by the structure's ability to prevent complete perforation by a projectile. A measure for the ballistic performance is the ballistic limit velocity V_{50}, which is the projectile impact velocity at which 50 % of specimens tested are completely perforated. The laminate properties are mainly optimised for their penetration resistance and the deformation of the laminate during the ballistic impact is generally ignored.

However, the current consensus from research on the ballistic impact response of laminated helmets is that the delamination response of the laminate might be a possible cause of head

injuries at impact velocities close to the ballistic limit. At these impact velocities, complete perforation of the helmet might be prevented, but the projectile's kinetic energy might be sufficient to separate the inner, non-perforated laminate layers from the remainder of the helmet. This separation of the helmet interior is a delamination process and the delaminated layers are generally referred to as the backplane. The backplane deformation depends on the amount of the projectile's kinetic energy dissipated during the penetration process. Fibre breakage, matrix cracking, through-thickness compressive and shear failure, and delamination are generally considered to be the major energy absorption modes in ballistically impacted laminates [1-4]. The impact of the delaminated backplane with the head of the helmet wearer is thought to be a potential cause of skull fracture and underlying brain damage.

In order to support further optimisation of the ballistic performance of laminated helmets, an improved understanding of the nature of the backplane delamination process and the subsequent impact of the backplane with the head of the helmet wearer is required. The complex response of composite laminates to ballistic impact together with the high cost and limited reproducibility of ballistic impact tests would render a completely experimental approach expensive and time consuming. Numerical modelling can provide a partial solution to this problem, since it allows a fast and relatively inexpensive means of gaining insight into the parameters determining the ballistic impact response of laminated composites.

The current research presents a numerical model capable of simulating the backplane response of laminated helmets. The model incorporates the four damage modes mentioned above. Both instantaneous and post-failure approaches were applied. The failure models were implemented in the LS-DYNA finite element code as user-defined material subroutines. The impact of fragment simulating projectiles (FSP) on woven aramid laminates was simulated. The effects of post-failure behaviour on the predicted penetration and backplane response are presented for impact velocities in the range 400-600 m/s.

FAILURE MODELS

Both instantaneous and post-failure models were used in the current research. Instantaneous failure models do not incorporate any residual load bearing capacity once the material is loaded beyond its strength. The stiffness values related to the failure direction are instantaneously reduced to zero once the strength is exceeded in a particular direction. However, composite materials generally exhibit some residual load bearing capacity once the loading surpasses the material strength. This residual load bearing capacity can be modelled with post-failure models, which define a more gradual decrease in the material stiffness once its strength has been exceeded. Recent work has shown that post-failure models can significantly improve damage predictions and reduce mesh sensitivity in models of transverse impacts on graphite [5-7] and aramid fibre-reinforced laminates [8-10].

The details of the instantaneous and post-failure models developed as part of the current study are outlined in the following. A distinction was made between intralaminar and interlaminar failure modes, and each of this type of failure mode was treated in a separate part of the software. The intralaminar failure modes included in-plane tensile failure (fibre breakage and matrix cracking) and through-thickness compressive and shear failure. These failure modes were modelled within the element constitutive routines and implemented in user-defined material subroutines. An element erosion algorithm was used to simulate cratering of the laminate by the projectile. The interlaminar failure mode included delamination, which was simulated using discrete interfaces inserted between layers of elements. Delamination

initiation and propagation were predicted using the normal and shear stresses in the interface. This treatment of delamination allowed the formation of a discrete delaminated backplane during the final stages of the laminate penetration process.

Intralaminar Failure

Instantaneous Failure Model

A strain-based instantaneous failure model, similar to the models by Hashin [11] and Chang and Chang [12,13], was developed for this project. In-plane tensile failure was predicted by relating either the longitudinal or transverse tensile strain to a corresponding critical strain. In case of unidirectional laminae this would imply that longitudinal tensile failure represents fibre breakage and transverse tensile failure represents matrix cracking. For woven fabric-reinforced composites, both longitudinal and transverse tensile failures correspond to fibre breakage. In-plane tensile failure was predicted by the following criteria:

$$f_i = \left(\frac{\varepsilon_{ii}}{\varepsilon_{fii}} \right)^{m_i} - r_i \geq 0 : \text{failure} \qquad (1)$$
$$< 0 : \text{no failure}$$

where $i=1,2$ denotes the in-plane directions, ε_{ii} are the in-plane tensile strains, ε_{fii} the corresponding failure strains, m_i the damage exponents, and r_i are the failure thresholds which are set equal to *1*. The effect of the damage exponent *m* will be discussed in the post-failure model. When in-plane tensile failure occurred in the *i*-direction, all stresses related to that direction (σ_{ij}, $j=1-3$) were set to zero instantaneously. In practice, the stresses were set to zero over *100* time steps to avoid numerical instability problems. Typical time steps in the simulations presented in this study were in the order of 12 μs.

During ballistic impact, the projectile will compress the composite material in the impacted area. This will lead to high compressive stresses under the projectile and high transverse shear stresses in the surrounding area. When these stresses exceed their related strength values, the projectile will punch a hole in the material. In order to be able to determine the relative contribution of the through-thickness compressive (crushing) and shear (punching) failure modes, different failure criteria were used to predict each of the through-thickness failure modes. Through-thickness compressive failure was predicted by the following criterion:

$$f_3 = \left(\frac{\varepsilon_{33}}{\varepsilon_{f33}} \right)^{m_3} - r_3 \geq 0 : \text{failure} \qquad (2)$$
$$< 0 : \text{no failure}$$

where ε_{33} is the through-thickness compressive strain, ε_{f33} the corresponding failure strain, m_3 the damage exponent, and r_3 is the failure threshold that was set equal to 1. Through-thickness shear failure was predicted using the following criterion:

$$f_4 = \left(\frac{\varepsilon_{23}}{\varepsilon_{f23}}\right)^{m_4} + \left(\frac{\varepsilon_{31}}{\varepsilon_{f31}}\right)^{m_4} - r_4 \geq 0 : \text{failure}$$
$$< 0 : \text{no failure} \tag{3}$$

where ε_{23} and ε_{31} are the through-thickness shear strains, ε_{f23} and ε_{f31} corresponding failure strains, m_4 the damage exponent, and r_4 the failure threshold which was set equal to 1. When through-thickness compressive or shear failure occurs, all stresses were instantaneously set to zero and the element was deleted from the mesh to simulate the formation of a crater by the projectile.

The failure strains used in the above failure criteria were obtained from the appropriate stress-strain relations for the composite laminate through:

$$\varepsilon_{fij} = \frac{S_{ij}}{E_{ij}} \tag{4}$$

where S_{ij} represent the strength values and E_{ij} are the corresponding stiffness values (Young's or shear modulus).

Post-Failure Model

The post-failure model used in this research was based on a Continuum Damage Mechanics approach, which characterises the onset and growth of damage by a decrease in stiffness of the material [14,15]. Matzenmiller et al. [16] developed a continuum damage mechanics model for anisotropic damage in elastic-brittle fibre-reinforced composites. Williams and Vaziri [7] first implemented this model as a user-defined subroutine in LS-DYNA and a similar approach was used for the current post-failure model. A set of damage variables w_i was introduced to relate the onset and growth of damage to stiffness losses in the material:

$$[\mathbf{C}] = \begin{bmatrix} \frac{1}{(1-w_{11})E_1} & \frac{-\nu_{21}}{E_2} & \frac{-\nu_{31}}{E_3} & 0 & 0 & 0 \\ \frac{-\nu_{12}}{E_1} & \frac{1}{(1-w_{22})E_2} & \frac{-\nu_{32}}{E_3} & 0 & 0 & 0 \\ \frac{-\nu_{13}}{E_1} & \frac{-\nu_{23}}{E_2} & \frac{1}{(1-w_{33})E_3} & 0 & 0 & 0 \\ 0 & 0 & 0 & \frac{1}{(1-w_{12})G_{12}} & 0 & 0 \\ 0 & 0 & 0 & 0 & \frac{1}{(1-w_{23})G_{23}} & 0 \\ 0 & 0 & 0 & 0 & 0 & \frac{1}{(1-w_{13})G_{31}} \end{bmatrix} \tag{5}$$

where $\boldsymbol{C}$ is the compliance matrix. The stiffness matrix is obtained by inverting the compliance matrix: $\boldsymbol{S}=\boldsymbol{C}^{-1}$. The following expressions were used for the damage variables:

$$w_{ij} = 1 - \exp\left[\frac{-1}{m_k e}\left(\frac{\varepsilon_{ii}}{\varepsilon_{fii}}\right)^{m_k}\right] \tag{6}$$

where k represents the failure mode that the damage variable w_{ij} is related to.

The same failure criteria as in the instantaneous failure model were used in the post-failure model. However, the damage thresholds, r_k, are no longer constants in the post-failure model, but are continuously increasing functions with increasing damage. The damage thresholds in the post-failure model can be thought of as being similar to the yield strength in plasticity theory with hardening. Consequently, the corresponding failure criteria, f_k, can be represented as damage surfaces in strain space, similar to the yield surface in plasticity theory. The post-failure model assumes linear elastic behaviour within the part of the strain space bounded by the damage thresholds. This means that both loading and unloading of the material are linear elastic as long as the damage thresholds are not exceeded. The non-linear elastic material behaviour is captured by the damage functions w_{ij} in case of damage growth. Damage growth will occur when the strain path crosses the damage surface ($f_k = 0$) and the strain increment has a non-zero component in the direction of the normal to the damage surface. The amount of damage growth in a particular damage mode is represented by an increase in the value of the damage function w_{ij} and the stiffness matrix, **S**, is updated accordingly. When the damage functions associated with the through-thickness compressive and shear failure modes (w_{3j}, $j=1\text{-}3$) are equal to 1, the corresponding element is removed from the mesh.

For illustrative purposes, the stress-strain response for the through-thickness compressive failure mode is shown in Fig. 1. As can be seen in Fig. 1a, the post-failure strength decreases more rapidly with strain with increasing values for m_3, and the post-failure model approaches the instantaneous failure model for high values of m_3. Fig. 1 shows that low values for m_3 or high values for S_{33} will lead to high compressive strains in the element before the element is deleted. These high compressive strains can lead to computational instabilities, such as negative volume and hourglassing problems. Therefore, care should be taken in the choice of m_3 and S_{33}.

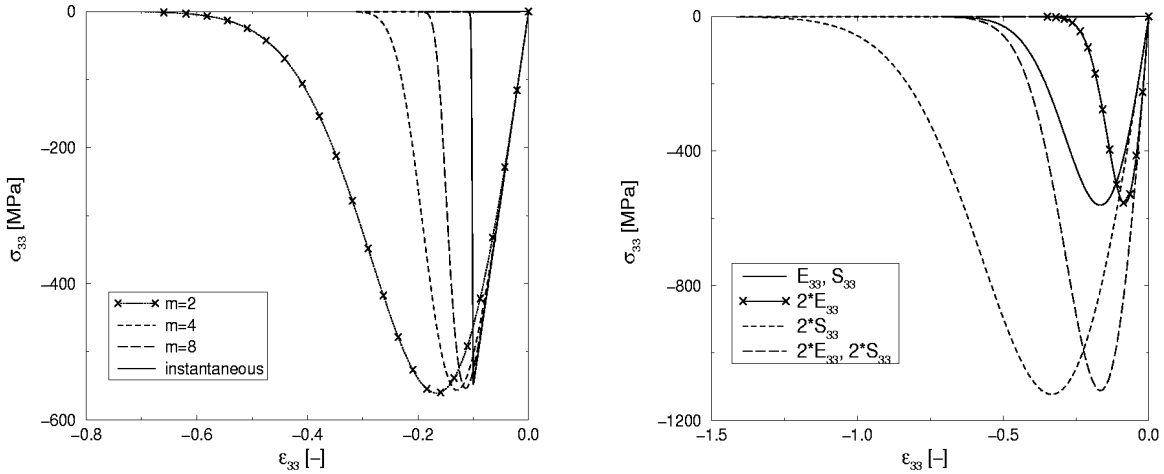

a: Effect of damage exponent m_3 b: Effect of stiffness E_{33} and strength S_{33}

Fig. 1: Post-failure stress-strain response

Interlaminar Failure

The interlaminar failure considered in this research consisted of delamination failure of adjacent plies. Delamination failure was implemented using a discrete delamination interface connecting adjacent element layers. The discrete delamination interface was based on the tie-

break contact algorithm in LS-DYNA. The interface rigidly connects the nodes of the adjacent layers until the following failure criterion is exceeded:

$$F_{delam} = \left(\frac{\sigma_n}{S_n}\right)^2 + \left(\frac{\sigma_s}{S_s}\right)^2 \begin{cases} \geq 0 : \text{failure} \\ < 0 : \text{no failure} \end{cases} \quad (7)$$

where σ_n and σ_s are the normal and shear interface stresses, respectively, and S_n and S_s are the corresponding strength values. When the delamination criterion is exceeded, the interface is allowed to separate, simulating inter-ply cracking. Modifications were made to the original tie-break interface to ensure that the contact definitions in the discrete delamination interface were properly updated when elements were eroded in the crater zone. A similar approach was undertaken by Hung et al. [17] who also modelled delamination in LS-DYNA with tie-break interfaces. Their numerical results were in good agreement with experimental data.

MODEL DESCRIPTION

Mesh

A finite element model of the FSP and the target panel were built using I-DEAS Masters Series, Version 6. The panel model consisted of 19 plies, each 0.5 mm thick, resulting in a total panel thickness of 9.5 mm. Each ply in the panel model was 1 element thick, resulting in 19 elements through the thickness of the panel. The panel model was impacted by a .22 calibre chisel nose FSP (MIL-P46593). The FSP was fabricated using 4340 steel, heat-treated to 28 Rc, and weighs 1.1 g. To reduce the computational time, only one quarter of the problem was modelled utilising symmetry. All components of the model were discretised using 8-node brick elements with single point integration. A typical mesh of the flat panel model with the FSP is shown in Fig. 2.

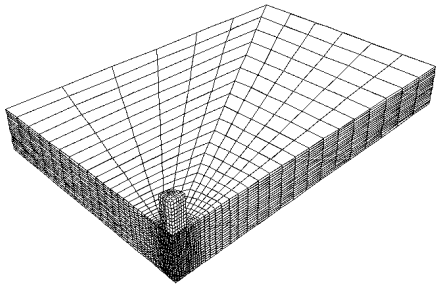

Fig. 2a: Composite panel model with FSP

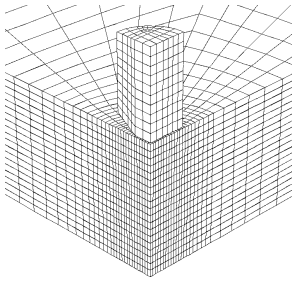

b: Close-up of impact area

Material Properties

The material properties for the woven fabric-reinforced aramid laminates were obtained from the literature. Most of this data was obtained under quasi-static loading conditions. The adopted values for the elastic and strength parameters in the numerical model are summarised in Table 1 and Table 2, respectively. These values were used as starting values. In ongoing work, the results from ballistic experiments on aramid panels and helmets will be used to obtain more realistic estimates for the material properties. The 4340 steel FSP material was modelled using a yield strength of 1,034 MPa and a hardening modulus of 685 MPa. Young's Modulus was taken as 207 GPa and Poisson's Ratio was 0.3. Ballistic impact tests showed that the ballistic limit for this target-projectile combination was about 600 m/s.

Table 1 Elastic properties adopted for aramid laminate in numerical model

Young's Moduli [GPa]		Shear Moduli [GPa]		Poisson's Ratio's [-]		Density [g/cm^3]
E_{11}, E_{22}	E_{33}	G_{12}	G_{23}, G_{31}	ν_{21}	ν_{31}, ν_{32}	ρ
18.5	6.0	0.77	1.36	0.25	0.33	1.23

Table 2 Strength properties adopted for aramid laminate in numerical model

Tensile [MPa]		Compressive [MPa]	Shear [MPa]	
S_{11}, S_{22}	S_n	S_{33}	S_{23}, S_{31}	S_s
740.0	34.5	1200.0	271.5	9.0

RESULTS

Fig. 3 and Fig. 4 show the predicted sequence of events for an FSP impacting an aramid panel at 500 m/s utilising the instantaneous and post-failure model, respectively. Both figures clearly show the formation of a crater in the panel model by deletion of elements that fail in either the through-thickness compressive or shear failure mode. Delamination occurs both adjacent to and ahead of the advancing FSP. The delaminations ahead of the FSP are thought to be caused by stress-waves preceding the FSP. It is clear from the two figures that the response of the instantaneous and post-failure models differs considerably. The predictions utilising the instantaneous failure model indicate that the panel is not capable of stopping the FSP. However, when the post-failure model is used, the numerical model predicts that complete perforation of the panel is prevented. Based on the experimentally determined ballistic limit of the considered target-projectile combination of 600 m/s, the post-failure model seems to provide a more realistic prediction.

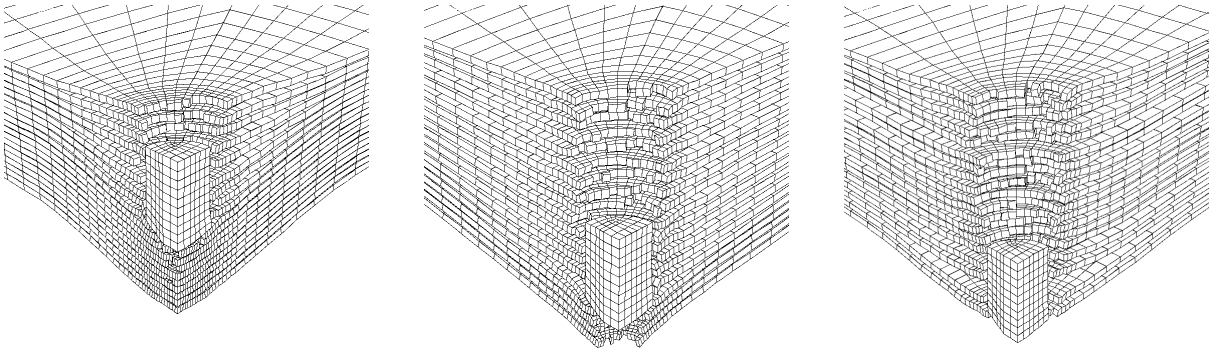

t=25 μs t=75 μs t=150 μs

Fig. 3: Instantaneous failure model, impact velocity of 500 m/s

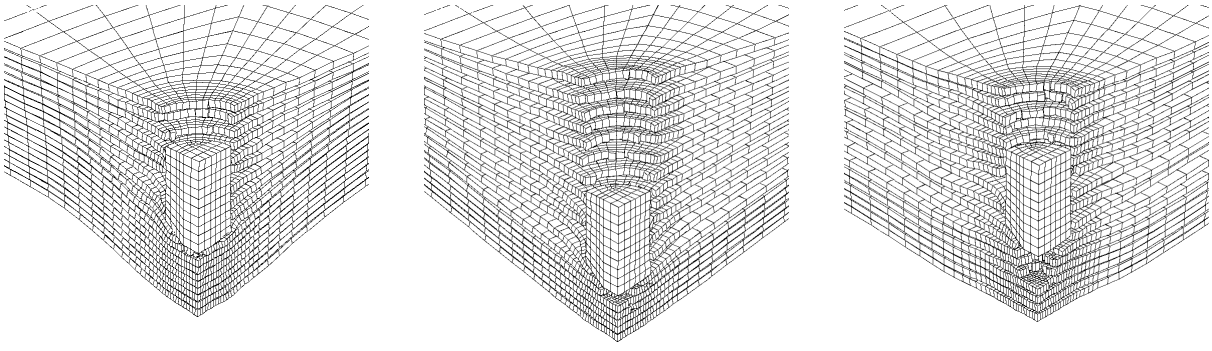

t=25 μs t=75 μs t=150 μs

Fig. 4: Post-failure model, impact velocity of 500 m/s

Fig. 5 shows the effect of the damage exponent *m* on the predicted ballistic response when the post-failure model is utilised in the simulations. The figure shows that the damage exponent corresponding to the through-thickness shear failure mode, m_4, has the most dominant effect on both the FSP velocity and backplane displacement time histories. This is in agreement with earlier findings presented in [10], where it was found that the through-thickness shear properties of the laminate governed the penetration process. However, it should be noted that the predicted response highly depends on the chosen material properties for the aramid laminate. Ongoing simulations of ballistic impact experiments will provide a clearer understanding of the parameters governing the ballistic impact response of the aramid laminate.

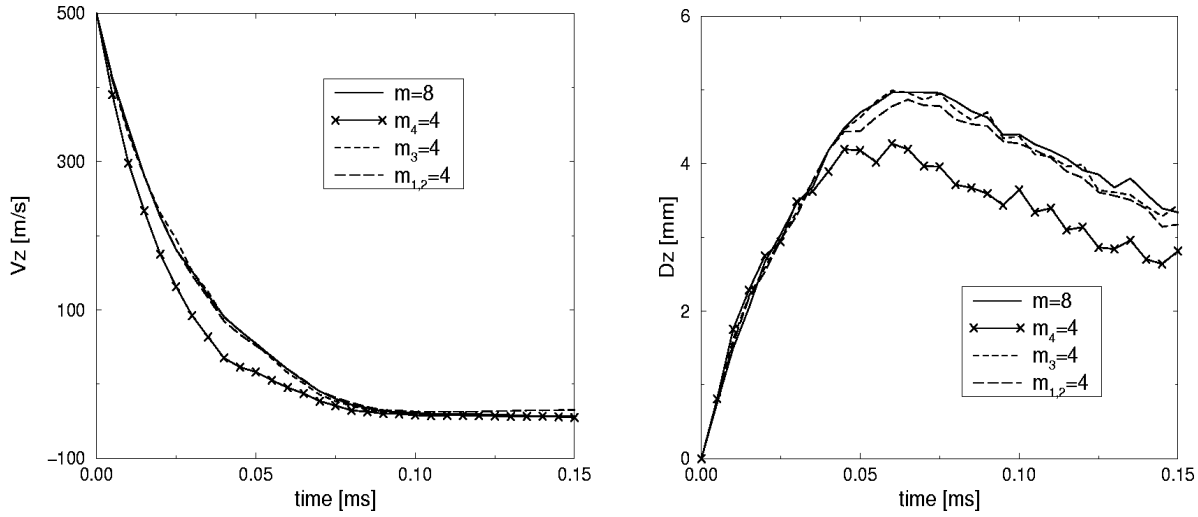

a) b)

Fig. 5: Effect of the damage exponent *m* on the response predicted by the post-failure model.
a) Effect of *m* on the FSP velocity time history;
b) Effect of *m* on backplane displacement time history

Fig. 6 shows the predicted projectile and backplane response for woven aramid laminates impacted by projectiles at 400-600 m/s, utilising the post-failure model. The FSP velocity time histories in Fig. 6a show that when the post-failure mode is used, the simulation predicts that the panel is capable of preventing complete perforation by projectiles impacting at 400 and 500 m/s. When the panel is impacted by an FSP at 600 m/s second, the simulation predicts that the FSP exits the panel with a residual velocity of 63 m/s. This is of particular interest, since the experimentally determined ballistic limit for this particular target-projectile combination lies around 600 m/s. Fig. 6b shows the predicted backplane displacement time histories for simulations incorporating the post-failure model. As can be seen from the figure, the backplane displacement increases with increasing impact velocity. The predicted backplane displacement resulting from the 600 m/s FSP impact is of less importance since the panel is completely perforated. It should be noted that Fig. 6b only shows trends and that the actual backplane response strongly depends on the material and damage properties of the lamina. The effects of these properties are not considered in this study and are subject of current research. Similar simulations utilising the instantaneous failure model predicted that the panel was only able to prevent the 400 m/s FSP from completely perforating the panel.

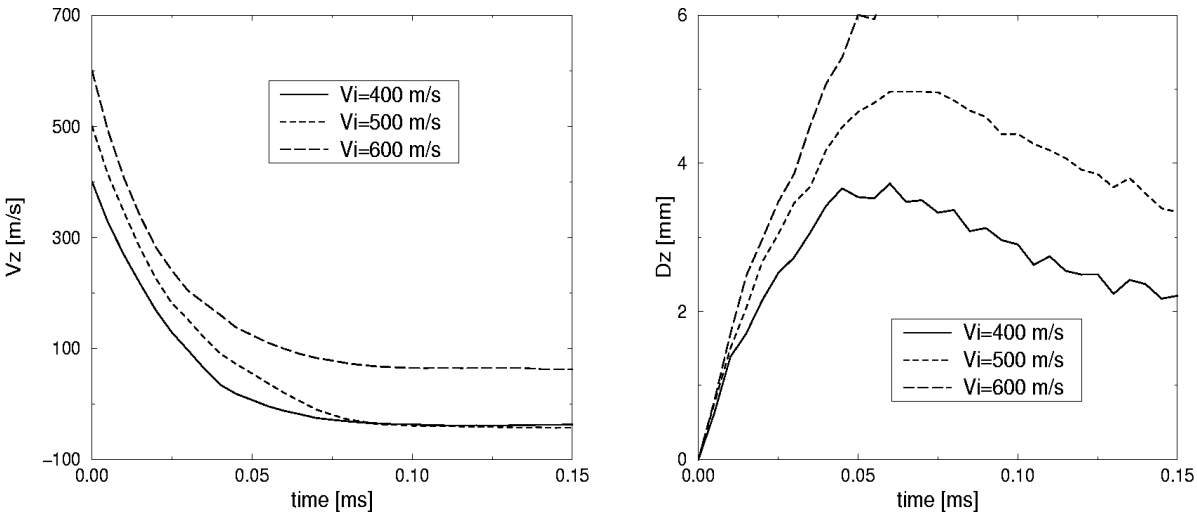

a) FSP velocity time histories b) Backplane displacement time histories

Fig. 6: FSP and Backplane response at impact velocities ranging 400-600 m/s, predicted utilising the post-failure model.

CONCLUSIONS

Simulations of the ballistic impact response of woven aramid laminates to FSP's impacting at 400-600 m/s showed that post-failure modelling had a considerable effect on the predicted impact response. Panel models incorporating the post-failure response were in most cases capable of stopping FSP impacts at velocities below the measured ballistic limit. Of particular interest is the 600 m/s impact case, since the experimentally determined ballistic limit of the aramid panels was found to be near this value. The results of the post-failure simulation at this impact velocity showed that the FSP exited the panel model with a residual velocity of 63 m/s. Simulations utilising the instantaneous failure model under predicted the ballistic performance of the woven aramid laminates.

The material properties used in this study were based on published results from quasi-static tests. The quasi-static values were used as starting values for the material properties required by the numerical model. Subsequent simulations of ballistic impact tests on aramid panels and helmets will be undertaken to provide more realistic estimates of the material parameters. Mesh refinement and a non-local damage approach are also the subjects of current research in order to avoid mesh-sensitivity issues.

REFERENCES

1. Langlie, S. and Cheng, W., "A High Velocity Impact Penetration Model for Thick Fiber-Reinforced Composites", *Proceedings of the ASME Pressure Vessels and Piping Conference*, Honolulu, HI, USA, July 23-27, 1989, pp. 151-158.

2. Zhu, G., Goldsmith, W. and Dharan, C.K.H., "Penetration of Laminated Kevlar by Projectiles – I. Experimental Investigation", *International Journal of Solids and Structures*, Vol.29, No. 4, 1992, pp. 399-420.

3. Zhu, G., Goldsmith, W. and Dharan, C.K.H., "Penetration of Laminated Kevlar by Projectiles – II. Analytical Model", *International Journal of Solids and Structures*, Vol.29, No. 4, 1992, pp. 421-436.

4. Lee, B.L., Song, J.W. and Ward, J.E., "Failure of Spectra Polyethylene Fiber-Reinforced Composites under Ballistic Impact Loading", *Journal of Composite Materials*, Vol. 28, No. 13, 1994, pp.1202-1226.

5. Majeed, O., Worswick, M.J., Straznicky, P.V., Poon, C., "Numerical Modelling of Transverse Impact on Composite Coupons", *Canadian Aeronautics and Space Journal*, Vol. 40, No. 3, 1994, pp. 99-106.

6. Straznicky, P.V., Poon, C., Worswick, M.J., Fuoss, E., Majeed, O., Vietinghoff, H., "Damage Resistance in Composite Materials", *Proceedings of ICCM-10*, Whistler, British Columbia, Canada, August 14-18, Vol. V: Structures, 1993, pp. 607-614.

7. Williams, K. and Vaziri, R., "Finite Element Analysis of the Impact Response of CFRP Composite Plates", *Proceedings of ICCM-10*, Whistler, British Columbia, Canada, August 14-18, Vol. V: Structures, 1993, pp. 647-654.

8. van Hoof, J., Worswick, M.J., Straznicky, P.V., Bolduc, M. and Tylko, S., "Parametric Study of a Finite Element Analysis of a Generic Protective Helmet Subjected to Ballistic Impact", *Proceedings of the 16th International Symposium on Ballistics*, San Francisco, CA, USA, Sept. 23-28, 1996, pp.143-152.

9. van Hoof, J., Worswick, M.J., Straznicky, P.V., Bolduc, M. and Tylko, S., "Finite Element Analysis of the Ballistic Impact Response of Composite Helmet Materials" *Proceedings of ICCM-11*, Gold Coast, Australia, July 14-18, 1996, pp. 532-541.

10. van Hoof, J., Worswick, M.J., Straznicky, P.V., Bolduc, M. and Tylko, S., "Simulation of the Ballistic Impact Response of Composite Helmets", *Proceedings of the 5th International LS-DYNA Users Conference*, Southfield, MI, USA, Sept. 21&22, 1998, H2.

11. Hashin, Z., "Failure Criteria for Unidirectional Fibre Composites", *Journal of Applied Mechanics*, Vol. 47, 1980, pp. 329-334.

12. Chang, F.K. and Chang, K.Y, "Post-Failure analysis of Bolted Composite Joints in Tension or Shear-Out Mode Failure", *Journal of Composite Materials*, Vol. 21, 1987a, pp. 809-833.

13. Chang, F.K. and Chang, K.Y, "A Progressive Damage Model for Laminated Composites Containing Stress Concentration", *Journal of Composite Materials*, Vol. 21, 1987b, pp. 834-855.

14. Kachanov, L.M., *Introduction to Continuum Damage Mechanics*, Martinus Nijhoff, Dordrecht, 1986.

15. Krajcinovic, D., *Damage Mechanics*, Elsevier Science, Amsterdam, The Netherlands, 1996.

16. Matzenmiller, A., Lubliner, J. and Taylor, R.L., "A Constitutive Model for Anisotropic Damage in Fiber-Composites", *Mechanics of Materials*, Vol. 20, 1995, pp. 125-152.

17. Hung, K.-S., Nilsson, L. and Zhong, Z.-H., "Numerical Studies on the Delamination Mechanism in Laminated Composites under Impact Loading", *Proceedings of ICCM-10*, Whistler, British Columbia, Canada, August 14-18, Vol. V: Structures, 1995, pp. 623-630.